we consider only asymptotic behaviors. Using the technique we used in subsection (b) we find

$$s(n_1,n_2,n_3,n_4)=\frac{1}{2\pi(eH_0)^{1/2}}\left\{7\zeta(3)-\frac{62}{3}\zeta(5)\rho+\frac{10541}{120}\zeta(7)\rho^2\right.$$

$$\left.-\frac{127}{60}\zeta(7)\rho^2\left[\frac{k^2}{4eH_0}((n_1-n_3)^2+(n_2-n_4)^2)+2\left(\frac{k^2}{4eH_0}\right)^2(n_1-n_3)^2(n_2-n_4)^2\right]\right\}, \quad \text{for} \quad \rho\ll 1, \tag{A27}$$

$$=\frac{1}{2\pi(eH_0)^{1/2}}4\rho^{-1}\ln(24\gamma\rho)\left\{[\ln(1+\sqrt{2})]^2\right.$$

$$\left.-\left[\frac{1}{2}+\frac{\ln(1+\sqrt{2})}{2\sqrt{2}}-(\ln(1+\sqrt{2}))^2\right]\frac{k^2}{4eH_0}((n_1-n_3)^2+(n_2-n_4)^2)\right\}$$

$$=\frac{1}{2\pi(eH_0)^{1/2}}4\rho^{-1}\ln(24\gamma\rho)\left\{0.77-0.04\frac{k^2}{4eH_0}[(n_1-n_3)^2+(n_2-n_4)^2]\right\}, \quad \text{for} \quad \rho\gg 1. \tag{A28}$$

Thus we see that in both limiting cases the effect of nonlocality of the kernel $K_1$ [i.e., the term containing the additional factor $(n_1-n_3)$ and/or $(n_2-n_4)$ in coefficient of $e^{-C(n_i)}$] is quite negligible. This fact suggests that it is a plausible approximation to replace nonlocal kernels by equivalent local ones, as we have done in the derivation of Eq. (35).

---

PHYSICAL REVIEW VOLUME 139, NUMBER 3A 2 AUGUST 1965

# Thermal Expansion and Other Anharmonic Properties of Crystals*

DUANE C. WALLACE
*Sandia Laboratory, Albuquerque, New Mexico*

(Received 1 March 1965)

The temperature dependences of the thermodynamic functions, as derived from lattice dynamics, are examined for the limit of low temperature and also for high temperatures (those above a high characteristic temperature). Particular attention is given to the effects of anharmonic terms in the lattice potential energy. Detailed calculations are reported for central-potential models for fcc, bcc, and hcp lattices. In particular, the normal-mode frequencies and Grüneisen parameters were calculated for a large number of points in the Brillouin zone as a function of volume; and the specific heat, compressibility, thermal-expansion coefficient, and macroscopic Grüneisen parameter were calculated as functions of temperature and volume. At fixed volume the isothermal compressibility shows little temperature dependence and the explicit anharmonic contribution is small; at zero pressure the compressibility increases with increasing temperature and the explicit anharmonic contribution is again small. The thermal-expansion coefficient exhibits similar behavior at high temperatures. The anharmonic specific heat is proportional to temperature at high temperatures, and also depends strongly on the volume. The effective Debye temperatures and the macroscopic Grüneisen parameters exhibit a wide variety of temperature and volume dependences. Approximations are developed for quantities which determine the behavior of thermodynamic functions at low and high temperatures, and approximate relations between several anharmonic properties are found. These approximations are tested by comparison with accurate calculations for the central-potential models.

## I. INTRODUCTION

THE purpose of the present paper is to report the results of a study of the thermodynamic properties of crystal lattices. The study is based on the lattice-dynamics free energy, and particular attention is given to the effects of the anharmonic terms in the lattice potential energy. Detailed calculations of thermodynamic functions for models based on central-potential interactions among the ions have been carried out for fcc, bcc, and hcp lattices. Even though the central-potential models are probably inadequate for an accurate description of most real materials, it is believed that the qualitative behavior of these models is representative of real crystals.

In order to study the statistical thermodynamics of a system, the first step is to define a mechanical problem of motion for the system. If the thermodynamic properties are to be studied as a function of configuration, then it is necessary to formulate the mechanical problem in such a way as to allow the configuration to be varied. Indeed, this is necessary in principle in order to define a

---

* This work was supported by the U. S. Atomic Energy Commission.

derivative of a thermodynamic function with respect to configuration. For a crystal composed of interacting ions, the configuration may be varied in the mechanical problem of motion by externally applied forces; this procedure has been discussed previously.[1]

The Hamiltonian for a conservative system of a finite crystal, composed of interacting ions plus externally applied forces, may be written

$$\begin{aligned}\mathcal{H}=U(\mathbf{r}_{nj})-W(\mathbf{r}_{nj})+\tfrac{1}{2}\textstyle\sum_{n,\rho} M_j(\dot{u}_{n\rho})^2\\ +\textstyle\sum_{n,\rho}(X_{n\rho}-f_{n\rho})u_{n\rho}+\tfrac{1}{2}\textstyle\sum_{nn',\rho\rho'} A_{n\rho,n'\rho'}u_{n\rho}u_{n'\rho'}\\ +(1/3!)\textstyle\sum_{nn'n'',\rho\rho'\rho''} B_{n\rho,n'\rho',n''\rho''}u_{n\rho}u_{n'\rho'}u_{n''\rho''}\\ +(1/4!)\textstyle\sum_{n\cdots n''',\rho\cdots\rho'''} C_{n\rho,n'\rho',n''\rho'',n'''\rho'''}\\ \times u_{n\rho}u_{n'\rho'}u_{n''\rho''}u_{n'''\rho'''}\,, \quad (1.1)\end{aligned}$$

and the equilibrium condition is

$$X_{n\rho}-f_{n\rho}=0\,, \quad \text{all } (n,\rho)\,. \qquad (1.2)$$

Here and in the following, the notation is the same as that used previously.[2–4] The symbol $n$ labels a unit cell, $j$ labels an ion in a unit cell, $i$ labels a Cartesian coordinate, $\nu$ stands for a pair of indices $(n,j)$, and $\rho$ stands for a pair of indices $(j,i)$. There are $J$ ions per unit cell, $M_j$ is the mass of an ion of type $j$, and $M_c$ is the total mass of ions in one unit cell. The equilibrium position of ion $(n,j)$ is $\mathbf{r}_{nj}=\mathbf{r}_n+\mathbf{r}_j$, the displacement of ion $(n,j)$ from its equilibrium position is $\mathbf{u}_{nj}$, and $\dot{\mathbf{u}}_{nj}$ is the time derivative of $\mathbf{u}_{nj}$. The function $U(\mathbf{r}_{nj})$ is the static lattice potential which results from interactions among the ions, and $W(\mathbf{r}_{nj})$ is the work done on the lattice by the external forces, measured from an arbitrary initial configuration of the lattice. The coefficients $X_{n\rho}$, $A_{n\rho,n'\rho'}$, etc., arise from interactions among the ions, and $f_{n\rho}$ is a component of the external force applied to ion $(n,j)$ in the equilibrium configuration.

Terms in the potential energy which are of higher order than quartic in the displacements are not considered here. In addition, the present work is restricted to the case of only surface forces applied to the crystal; hence, $f_{n\rho}$ vanish in the interior and (1.2) becomes

$$X_{n\rho}=0\,, \quad \text{for all } (n,j) \text{ in the interior.} \qquad (1.3)$$

Surface effects may be eliminated by considering a macrocrystal containing $N$ unit cells in the interior, and the harmonic Hamiltonian may be diagonalized with the aid of the cyclic boundary condition. Hereafter the origin of coordinates is taken at a cell vector in the interior, i.e., $\mathbf{r}_n=0$ for $n=0$, and surface effects are eliminated from all lattice sums. The harmonic Hamiltonian represents a generalized eigenvalue problem, whose solution is given in terms of the $\mathbf{a}_\mathbf{k}$ matrices and the vectors $\mathbf{v}_{\mathbf{k},s}$.[5]

$$\begin{aligned}a_{\mathbf{k},\rho\rho'}=\textstyle\sum_{n'} A_{0\rho,n'\rho'}\\ \times\exp[i\mathbf{k}\cdot(\mathbf{r}_{n'j'}-\mathbf{r}_j)]\,, \quad (1.4)\end{aligned}$$

$$\textstyle\sum_{\rho\rho'} v_{-\mathbf{k},\rho s}a_{\mathbf{k},\rho\rho'}v_{\mathbf{k},\rho's'}=M_c(\omega_{\mathbf{k}s})^2\delta_{ss'}\,, \qquad (1.5)$$

$$\textstyle\sum_{\rho} M_j v_{\mathbf{k},\rho s}v_{-\mathbf{k},\rho s'}=M_c\delta_{ss'}(\text{orthogonality})\,, \qquad (1.6)$$

$$M_j\textstyle\sum_{s} v_{\mathbf{k},\rho s}v_{-\mathbf{k},\rho' s}=M_c\delta_{\rho\rho'}(\text{completeness})\,, \qquad (1.7)$$

where $\mathbf{v}_{-\mathbf{k},s}=\mathbf{v}_{\mathbf{k},s}{}^*$ has been taken. There are $N$ wave vectors $\mathbf{k}$ distributed uniformly over the Brillouin zone, and there are $3J$ values of the polarization index $s$.

Throughout the present paper it is considered that the anharmonic terms in (1.1), namely those cubic and quartic in the displacements, may be treated as a perturbation. The Helmholtz free energy $F$ is a function of configuration and temperature $T$, and may be written

$$F=F_H+F_A\,, \qquad (1.8)$$

$$\begin{aligned}F_H=U+NJE_H\\ +KT\textstyle\sum_{\mathbf{k},s}\ln[1-\exp(-\hbar\omega_{\mathbf{k}s}/KT)]\,, \quad (1.9)\end{aligned}$$

$$E_H=(NJ)^{-1}\textstyle\sum_{\mathbf{k},s}\tfrac{1}{2}\hbar\omega_{\mathbf{k}s}\,. \qquad (1.10)$$

Here $U$ is the static lattice potential, as in (1.1), and $E_H$ is the harmonic zero-point vibrational energy per ion. $U$ and $\omega_{\mathbf{k}s}$ are functions of the configuration only. The quantum derivation of $F_A$ has been given by Ludwig[6]; the expression is complicated and need not be given here.

The thermodynamic functions may be obtained from $F$ by means of well-known formulas.[7]

$$k^{-1}=V(\partial^2F/\partial V^2)_T\,, \qquad (1.11)$$

$$\beta=-k(\partial^2F/\partial T\partial V)_{V,T}\,, \qquad (1.12)$$

$$C=-T(\partial^2F/\partial T^2)_V\,, \qquad (1.13)$$

where $V$ is the volume of the macrocrystal, containing $NJ$ ions, for which the free energy has been computed, $k$ is the isothermal compressibility, $\beta$ is the thermal expansion coefficient, and $C$ is the specific heat at constant volume. A macroscopic Gruneisen parameter is defined as

$$\gamma=\beta V/kC\,. \qquad (1.14)$$

A subscript $A$ will be used to specify the explicit anharmonic contribution to a function, namely that contribution arising from $F_A$, while a subscript $H$ denotes contributions arising from $F_H$, including the volume derivatives of $F_H$. These latter terms are quasiharmonic terms.

---

[1] D. C. Wallace, Rev. Mod. Phys. **37**, 57 (1965).

[2] D. C. Wallace, Phys. Rev. **131**, 2046 (1963).

[3] D. C. Wallace, Phys. Rev. **133**, A153 (1964).

[4] D. C. Wallace and J. L. Patrick, Phys. Rev. **137**, A152 (1965).

[5] In Refs. 1 and 4, the $M_c\omega_{\mathbf{k}s}{}^2$ were referred to as the eigenvalues of $\mathbf{a}_\mathbf{k}$ matrices. Since the transformation which diagonalizes $\mathbf{a}_\mathbf{k}$, according to (1.5), is nonunitary by virtue of (1.6) and (1.7), it is more appropriate to refer to $M_c\omega_{\mathbf{k}s}{}^2$ as the eigenvalues of matrices whose elements are $(M_c{}^2/M_jM_{j'})^{1/2}a_{\mathbf{k},\rho\rho'}$.

[6] W. Ludwig, J. Phys. Chem. Solids 4, 283 (1958).

[7] Equations (1.11)–(1.13) are derivable from the definitions of $F$, $C$, $\beta$, and $k$ as given in any standard text; for example, R. Fowler and E. A. Guggenheim, *Statistical Thermodynamics* (Cambridge University Press, Cambridge, England, 1939).

## II. LOW- AND HIGH-TEMPERATURE BEHAVIOR

### Low Temperature

In order to determine the temperature dependence of the free energy in the limit of low temperature, it is necessary to use the method of long waves,[8] since it is the **k** dependence of appropriate integrands which inevitably determines the temperature dependence. According to the method of long waves, for a given direction of **k** there are three acoustic modes for which $\omega_s(\theta,\phi)=c_s(\theta,\phi)|\mathbf{k}|$, $s=1, 2, 3$, where $(\theta,\phi)$ are the angles which specify the direction of **k**. The asymptotic low-temperature expressions for the free energy may then be written

$$F_{Ht}=U+NJE_H-NJ(\pi^4/5)(K\theta_{H0})(T/\theta_{H0})^4, \quad (2.1)$$

$$F_{At}=gT^4, \quad (2.2)$$

where $\theta_{H0}$ is the harmonic Debye temperature at $T=0$ and is given by

$$(K\theta_{H0})^{-3}=(V/72NJ\hbar^3\pi^3)\sum_s \int d\Omega[c_s(\theta,\phi)]^{-3}. \quad (2.3)$$

In (2.3) the $\sum_s$ is carried out over the three acoustic branches and the $\int d\Omega$ is carried out over all angles $\theta$, $\phi$. Here and in the following a subscript $t$ denotes a low-temperature form, while a subscript 0 denotes a $T=0$ form. The coefficient $g$, which depends on the configuration only, is quite complicated, even for primitive lattices. The form (2.1) has been known since 1912,[9] while the rigorous proof of (2.2) has been given only recently.[3]

With the aid of (1.11)–(1.13), and keeping only the lowest order temperature dependence at low temperature, the following results are obtained:

$$k_t=k_0+O(T^4), \quad (2.4)$$

$$\beta_t=-k_0T^3[NJ(12\pi^4/5)(K/\theta_{H0}^4)\times(d\theta_{H0}/dV)+4(dg/dV)], \quad (2.5)$$

$$C_t=3NJKT^3[(4\pi^4/5\theta_{H0}^3)-4(g/NJK)], \quad (2.6)$$

where

$$k_0^{-1}=V(d^2U/dV^2)+NJV(d^2E_H/dV^2). \quad (2.7)$$

The relative contribution to $k_t$ of the term of order $T^4$ is extremely small at low temperatures and will be neglected hereafter. In addition, the explicit anharmonic contribution to $k_0^{-1}$ has been omitted in (2.7); this contribution is negligible for purposes of the present study (<0.01%).

Since $F_{Ht}$ and $F_{At}$ both go as $T^4$, they both give contributions with the same temperature dependence to each thermodynamic function. Thus the explicit anharmonic contribution to each function may be considered small at low temperatures. It is convenient to define a quasiharmonic Grüneisen parameter $\gamma_{H0}$ by neglecting the explicit anharmonic contributions; this gives the well-known quantity

$$\gamma_{H0}=-d\ln\theta_{H0}/d\ln V, \quad =\langle c_s^{-3}(\tfrac{1}{3}+\gamma_s)\rangle/\langle c_s^{-3}\rangle, \quad (2.8)$$

where the brackets ⟨ ⟩ indicate an average over acoustic modes and over angles, and where

$$\gamma_s=-d\ln c_s/d\ln V. \quad (2.9)$$

### High Temperature

The asymptotic high-temperature expressions for the free energy are

$$F_{HT}=U+KT\sum_{\mathbf{k},s}[\ln(\hbar\omega_{\mathbf{k}s}/KT)+(1/24)(\hbar\omega_{\mathbf{k}s}/KT)^2-\cdots], \quad (2.10)$$

$$F_{AT}=GT^2+O(T^{-2})+\cdots, \quad (2.11)$$

where here and in the following a subscript $T$ denotes a high-temperature form. The leading $T^2$ dependence of $F_{AT}$ was first shown by Born and Brody[10]; the coefficient $G$ depends on the configuration only.

In contrast to the low-temperature limit, the high-temperature contributions $F_{HT}$ and $F_{AT}$ do not have the same leading temperature dependence. The relative contribution to each thermodynamic function which arises explicitly from $F_{AT}$ increases with increasing $T$, and consequently cannot be considered small in general. The high-temperature behavior can be studied by dropping all contributions which decrease with increasing $T$; this procedure gives

$$k_T^{-1}=V(d^2U/dV^2)[1+\beta_3T+\beta_4T^2], \quad (2.12)$$

$$\beta_T=\beta_1(1-\beta_2T)[1+\beta_3T+\beta_4T^2]^{-1}, \quad (2.13)$$

$$C_T=3NJK[1-\beta_5T], \quad (2.14)$$

where

$$\beta_1=[K\textstyle\sum_{\mathbf{k},s}\gamma_{\mathbf{k}s}][V^2(d^2U/dV^2)]^{-1}, \quad (2.15)$$

$$\beta_2=2(VdG/dV)[K\textstyle\sum_{\mathbf{k},s}\gamma_{\mathbf{k}s}]^{-1}, \quad (2.16)$$

$$\beta_3=[K\textstyle\sum_{\mathbf{k},s}\xi_{\mathbf{k}s}][V^2(d^2U/dV^2)]^{-1}, \quad (2.17)$$

$$\beta_4=[V^2(d^2G/dV^2)][V^2(d^2U/dV^2)]^{-1}, \quad (2.18)$$

$$\beta_5=2G/3NJK, \quad (2.19)$$

$$\gamma_{\mathbf{k}s}=-(V/\omega_{\mathbf{k}s})(d\omega_{\mathbf{k}s}/dV), \quad (2.20)$$

$$\xi_{\mathbf{k}s}=(V^2/\omega_{\mathbf{k}s})(d^2\omega_{\mathbf{k}s}/dV^2)-\gamma_{\mathbf{k}s}^2. \quad (2.21)$$

The expressions (2.12)–(2.14) are expected to apply at temperatures somewhat above a high-temperature characteristic temperature, such as $\theta_{H\infty}$ (defined below), but not so high that $F_{AT}$ becomes comparable to $F_{HT}$.

The definition of $\theta_{H\infty}$ is based on the high-temperature

---

[8] M. Born and K. Huang, *Dynamical Theory of Crystal Lattices* (Clarendon Press, Oxford, England, 1954).

[9] P. Debye, Ann. Physik **39**, 789 (1912).

[10] M. Born and E. Brody, Z. Physik **6**, 132 (1921).

expansion for the harmonic specific heat.[11]

$$C_{HT}=3NJK[1-(1/20)(\theta_{H\infty}/T)^2+\cdots], \quad (2.22)$$

$$(K\theta_{H\infty})^2=(5\hbar^2/3)[(3NJ)^{-1}\sum_{\mathbf{k},s}(\omega_{\mathbf{k}s})^2]. \quad (2.23)$$

The macroscopic Grüneisen parameter has the following properties at high temperature.

$$\gamma_T=\gamma_{H\infty}(1-\beta_2T)(1-\beta_5T)^{-1}, \quad (2.24)$$

$$\gamma_{H\infty}=(3NJ)^{-1}\sum_{\mathbf{k},s}\gamma_{\mathbf{k}s}, \quad (2.25)$$

$$(V/\gamma_{H\infty})(d\gamma_{H\infty}/dV)=1-(3NJ\gamma_{H\infty})^{-1}\sum_{\mathbf{k},s}\xi_{\mathbf{k}s}. \quad (2.26)$$

Note that in the limit $\mathbf{k}=0$ for the acoustic modes,

$$\gamma_{\mathbf{k}s}=\gamma_s+\tfrac{1}{3}. \quad (2.27)$$

## III. METHODS OF CALCULATION

### Central-Potential Models

The numerical calculations of the present paper are restricted to the following: one or two ions per unit cell with all masses the same (i.e., all $M_j=M$); uniform volume changes, i.e., with no change in the relative unit cell parameters; and all pairs of ions interacting according to a given central potential. The fcc and hcp lattices are treated for eight Lennard-Jones potentials, abbreviated LJ$(\alpha,\beta)$ where $\alpha$ and $\beta$ are exponents appearing in the potential form. The bcc lattice is treated for LJ(6,4) and for three Rydberg potentials, abbreviated R$(\gamma\epsilon_0/\sqrt{3})$. These models are discussed in detail in a previous paper.[4]

In particular, $\epsilon$ is the nearest-neighbor distance, $\epsilon_0$ is the value for which the static lattice potential $U$ is a minimum, and $\sigma$ is defined by

$$\sigma=(\epsilon-\epsilon_0)/\epsilon_0. \quad (3.1)$$

Note that $\epsilon_0$ is a first approximation to the nearest-neighbor distance at temperature and pressure equal zero; a second approximation[4] is $(1+\kappa)\epsilon_0$ where $\kappa$ is a small parameter defined in (3.19) below. All volume derivatives were transformed to $\sigma$ derivatives in the numerical work. The $\omega_{\mathbf{k}s}$ were obtained as a function of $\sigma$ by diagonalizing the $\mathbf{a}_\mathbf{k}$ matrices, whose $\sigma$ dependence was calculated according to

$$\mathbf{a}_\mathbf{k}(\sigma)=\mathbf{a}_\mathbf{k}(\sigma=0)+\sigma[(d\mathbf{a}_\mathbf{k}/d\sigma)(\sigma=0)]+\cdots. \quad (3.2)$$

The series (3.2) was calculated to order $\sigma^2$ in all cases. At any $\sigma$, the derivatives of the $\omega_{\mathbf{k}s}$ were obtained with the aid of the Hellmann-Feynman theorem[12]:

$$d(M\omega_{\mathbf{k}s}^2)/d\sigma=\sum_{\rho\rho'}v_{-\mathbf{k},\rho s}(d\mathbf{a}_\mathbf{k}/d\sigma)_{\rho\rho'}v_{\mathbf{k},\rho's}. \quad (3.3)$$

For two ions per unit cell the dynamical matrices and their $\sigma$ derivatives were transformed to real-symmetric form.[2] Quantities containing first derivatives of $\omega_{\mathbf{k}s}$, such as $\beta_1$ of (2.15), were computed by direct summation over the reduced portion of the Brillouin zone for several values of $\sigma$ for each model. Quantities containing second derivatives of $\omega_{\mathbf{k}s}$, such as $\beta_3$ of (2.17), were obtained from the $\sigma$ dependence of quantities which contain only the first derivatives. The required volume derivatives of $G$ were computed approximately, as discussed in Sec. V.

### Method of Long Waves

The object is to find the real-symmetric 3×3 matrix $\boldsymbol{\lambda}(\theta,\phi)$, whose eigenvalues are $M[c_s(\theta,\phi)]^2$, $s=1, 2, 3$. For a primitive lattice, an expansion of $\mathbf{a}_\mathbf{k}$ to order $\mathbf{k}^2$ for small $\mathbf{k}$ yields $\boldsymbol{\lambda}$ directly.[3]

$$\boldsymbol{\lambda}(\theta,\phi)=\mathbf{a}_\mathbf{k}/\mathbf{k}^2, \quad \text{to order } \mathbf{k}^2; \quad (3.4)$$

$$[\boldsymbol{\lambda}(\theta,\phi)]_{ii'}=-\tfrac{1}{2}\sum_n A_{0i,ni'}(\hat{k}\cdot\mathbf{r}_n)^2. \quad (3.5)$$

Here $\hat{k}=\hat{k}(\theta,\phi)$ is a unit vector in the direction of $\mathbf{k}$.

For the special case of two ions per unit cell with all masses the same and a single central potential between all pairs of ions, it is possible to find a simple expression for $\boldsymbol{\lambda}$. The $\mathbf{a}_\mathbf{k}$ matrix, to order $\mathbf{k}^2$, may be written

$$\mathbf{a}_\mathbf{k}=\begin{pmatrix}\mathbf{P} & \mathbf{Q}\\ \mathbf{Q}^* & \mathbf{P}\end{pmatrix}, \quad (3.6)$$

where

$$\mathbf{P}=\mathbf{P}_0+\tfrac{1}{2}\mathbf{k}^2\mathbf{P}_2, \quad (3.7)$$

$$\mathbf{Q}=-\mathbf{P}_0+i|\mathbf{k}|\mathbf{Q}_1+\tfrac{1}{2}\mathbf{k}^2\mathbf{Q}_2, \quad (3.8)$$

$$(\mathbf{P}_0)_{ii'}=-\sum_n A_{0ji,nj'i'}, \quad j\neq j', \quad (3.9)$$

$$(\mathbf{P}_2)_{ii'}=-\sum_n A_{0ji,nji'}(\hat{k}\cdot\mathbf{r}_n)^2, \quad (3.10)$$

$$(\mathbf{Q}_1)_{ii'}=\sum_n A_{0ji,nj'i'}[\hat{k}\cdot(\mathbf{r}_{nj'}-\mathbf{r}_j)], \quad j\neq j', \quad (3.11)$$

$$(\mathbf{Q}_2)_{ii'}=-\sum_n A_{0ji,nj'i'}[\hat{k}\cdot(\mathbf{r}_{nj'}-\mathbf{r}_j)]^2, \quad j\neq j'. \quad (3.12)$$

$\mathbf{P}_0$, $\mathbf{P}_2$, $\mathbf{Q}_1$, and $\mathbf{Q}_2$ are all real-symmetric 3×3 matrices. Now $\mathbf{a}_\mathbf{k}$ of (3.6) may be reduced to order $\mathbf{k}^2$ by a straightforward application of matrix perturbation methods, i.e., $\mathbf{a}_\mathbf{k}$ is transformed by a unitary transformation so that the off-diagonal submatrices are zero ot order $\mathbf{k}^2$. The real-symmetric 3×3 matrices along the diagonal of the reduced form then give the acoustic and optical frequencies as eigenvalues. In particular

$$\boldsymbol{\lambda}(\theta,\phi)=\tfrac{1}{2}(\mathbf{P}_2+\mathbf{Q}_2-\mathbf{Q}_1\mathbf{P}_0^{-1}\mathbf{Q}_1), \quad (3.13)$$

$$\boldsymbol{\lambda}_{\text{opt}}(\theta,\phi)=2\mathbf{P}_0+\tfrac{1}{2}\mathbf{k}^2[\mathbf{P}_2-\mathbf{Q}_2 +\tfrac{1}{2}(\mathbf{P}_0^{-1}\mathbf{Q}_1\mathbf{Q}_1+\mathbf{Q}_1\mathbf{Q}_1\mathbf{P}_0^{-1})]. \quad (3.14)$$

The eigenvalues of $\boldsymbol{\lambda}(\theta,\phi)$ are $M[c_s(\theta,\phi)]^2$; the eigenvalues of $\boldsymbol{\lambda}_{\text{opt}}(\theta,\phi)$ are $M\omega_s^2$ for the optical branches.

The elements of the matrices $\boldsymbol{\lambda}$ and $(d\boldsymbol{\lambda}/d\sigma)$ are simply expressed in terms of previously tabulated lattice sums.[4] These matrices were computed for all the models at $\sigma=0$. The $\gamma_s$, defined by (2.9), were computed by an equation analogous to (3.3). The low-temperature in-

---

[11] See, for example, G. K. Horton and H. Schiff, Proc. Roy. Soc. (London) **A250**, 248 (1959).

[12] H. Hellmann, *Einfuhrung in die Quantenchemie* (Franz Deuticke, Leipzig, 1937); R. P. Feynman, Phys. Rev. **56**, 340 (1939).

tegrals were carried out numerically by taking $5(10^3)$ points in the double-angle integrations; this gave all integrals accurate to 2 parts in $10^4$.

### Reduced Quantities

All calculations were carried out in terms of reduced quantities, which are denoted by a superscript bar. Some needed definitions are

$$U(\sigma=0)=NJD,\ \text{defining } D; \tag{3.15}$$

$$V(\sigma=0)=NJV_a,\ \text{defining } V_a \text{ as the volume per ion at } \sigma=0; \tag{3.16}$$

$$\eta_{\mathbf{k}s}=M(\omega_{\mathbf{k}s})^2; \tag{3.17}$$

$$\Omega_\mu=(3NJ)^{-1}\sum\nolimits_{\mathbf{k},s}(\eta_{\mathbf{k}s})^{\mu/2}; \tag{3.18}$$

$$\kappa=(\hbar^2/MD\epsilon_0^2)^{1/2},\ \text{a dimensionless small parameter}. \tag{3.19}$$

For most elements, $0.5<(10^3)\kappa<5.0$.[4] Some of the reduced quantities of the present work are as follows:

$$\begin{gathered}\bar\eta_{\mathbf{k}s}=(\epsilon_0^2/D)\eta_{\mathbf{k}s},\quad \bar\Omega_\mu=(\epsilon_0^2/D)^{\mu/2}\Omega_\mu;\\ \bar F_H=F_H/NJD,\quad \bar E_H=E_H/D;\\ \bar G=(D/NJK^2)G;\\ \bar\theta_H=K\theta_H/D;\\ \bar C=C/NJK;\\ \bar k=(D/V_a)k;\\ \bar\beta=(D/K)\beta,\quad \text{similarly for } \bar\beta_1,\bar\beta_2,\bar\beta_3,\bar\beta_5;\\ \bar\beta_4=(D/K)^2\beta_4.\end{gathered} \tag{3.20}$$

The transformation of all equations to reduced equations is straightforward; for example,

$$\bar\theta_{H\infty}=\kappa[(5/3)\bar\Omega_2]^{1/2}, \tag{3.21}$$

$$\bar E_H=\tfrac{3}{2}\kappa\bar\Omega_1, \tag{3.22}$$

$$(\bar k_0)^{-1}=V^2(d^2\bar U/dV^2)+V^2(d^2\bar E_H/dV^2),\quad \text{at } \sigma=0. \tag{3.23}$$

In addition to the low- and high-temperature studies, detailed calculations were carried out for intermediate temperatures with the aid of the reduced temperature $\bar T$.

$$\bar T=T/\theta_{H\infty},\quad \theta_{H\infty} \text{ evaluated at } \sigma=0. \tag{3.24}$$

With the aid of (3.17), (3.20), and (3.21) it follows that

$$\hbar\omega_{\mathbf{k}s}/KT=[3\bar\eta_{\mathbf{k}s}/5\bar\Omega_2(\sigma=0)]^{1/2}\bar T^{-1},\quad \text{for any } \sigma; \tag{3.25}$$

the quantity in (3.25) is needed for all intermediate temperature calculations. The functions $\bar F_H$, $\bar C_H$, $\bar\beta_H$, and $\gamma_H$ were computed for each lattice model for $\sigma=-0.02, -0.01,\cdots,0.06$ and for $\bar T=0.04, 0.08,\cdots, 4.00$. The calculations were carried out by direct summation over the reduced portion of the Brillouin zone[4]; all such sums are in error by no more than 1 part in $10^3$ for $\bar T\geq 0.20$.

All numerical work was done with the aid of a CDC-1604 digital computer. The computer was also used for extensive studies of the accuracies of representative sums and integrals.

## IV. RESULTS

### Eigenvalues and Gruneisen Parameters

Figures 1–6 are representative graphs of $\bar\eta_{\mathbf{k}s}$ and $\gamma_{\mathbf{k}s}$ along certain lines in the Brillouin zones for the models

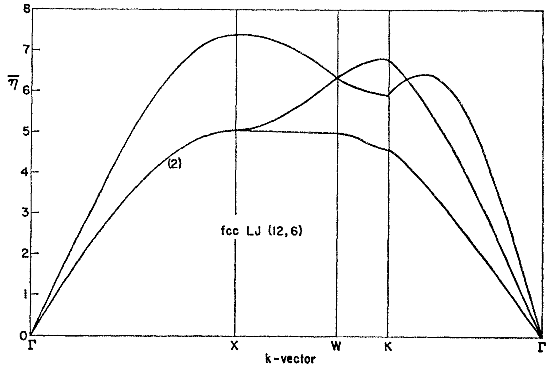

FIG. 1. Some values of $\bar\eta_{\mathbf{k}s}$ for fcc lattice, LJ(12,6) potential, at $\sigma=0$. The line marked (2) is doubly degenerate.

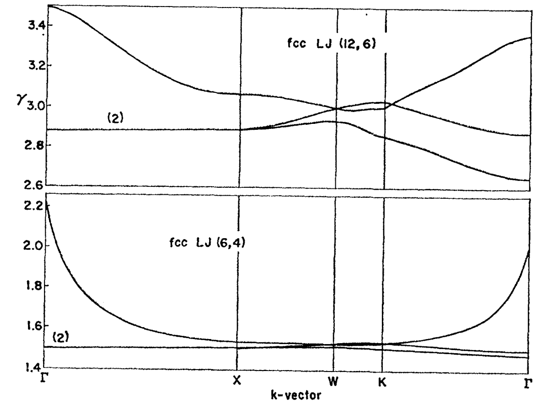

FIG. 2. Some values of $\gamma_{\mathbf{k}s}$ for fcc lattice, LJ(12,6) potential (top graph) and LJ(6,4) potential (bottom graph), at $\sigma=0$. The lines marked (2) are doubly degenerate.

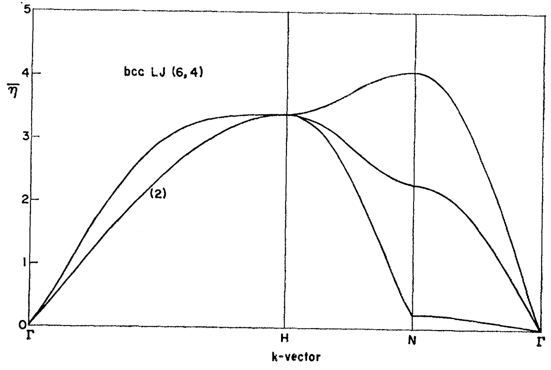

FIG. 3. Some values of $\bar\eta_{\mathbf{k}s}$ for bcc lattice, LJ(6,4) potential, at $\sigma=0$. The line marked (2) is doubly degenerate.

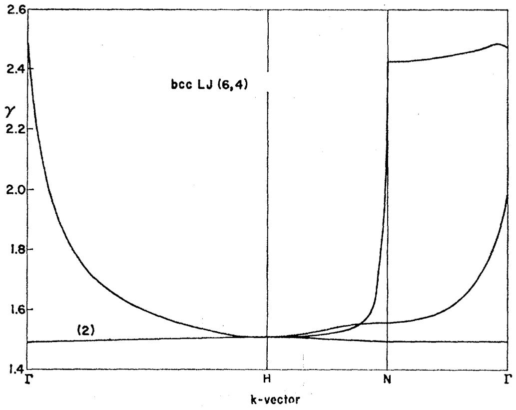

FIG. 4. Some values of $\gamma_{\mathbf{k}s}$ for bcc lattice, LJ(6,4) potential, at $\sigma=0$. The line marked (2) is doubly degenerate.

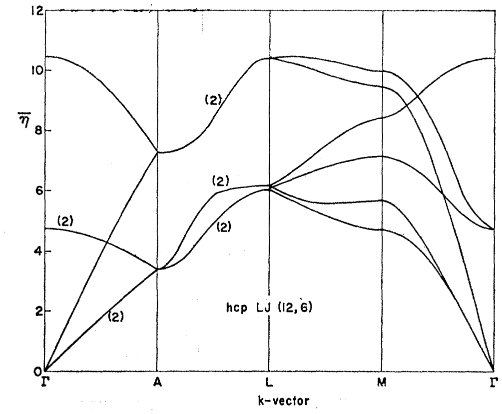

FIG. 5. Some values of $\bar{\eta}_{\mathbf{k}s}$ for hcp lattice, LJ(12,6) potential, at $\sigma=0$. The lines marked (2) are doubly degenerate.

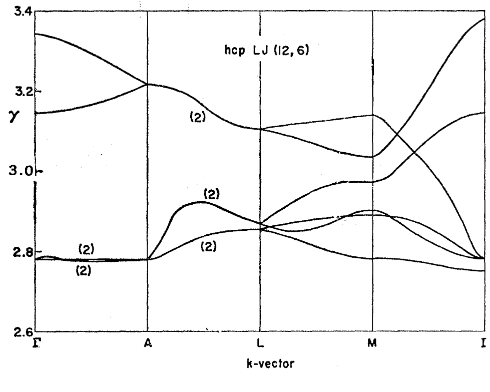

FIG. 6. Some values of $\gamma_{\mathbf{k}s}$ for hcp lattice, LJ(12,6) potential, at $\sigma=0$. The lines marked (2) are doubly degenerate.

of the present paper. The values shown are all for $\sigma=0$. For the fcc lattice, the curves of $\bar{\eta}_{\mathbf{k}s}$ for all eight Lennard-Jones potentials are nearly identical when scaled so as to coincide at any particular **k** vector. The various models for bcc show qualitative similarity in the $\bar{\eta}_{\mathbf{k}s}$; for example, the frequencies are small for one branch for **k** in the [011] and nearby directions. This property of the central potential bcc models has been discussed previously in connection with the stability of such models,[4] and further effects of these small frequencies will be noted below. The $\bar{\eta}_{\mathbf{k}s}$ curves for the eight hcp models are again quite similar when appropriately scaled. An interesting result for the hcp is that along the line *AL* on the zone surface there are three lines for the $\bar{\eta}_{\mathbf{k}s}$ spectrum, each line being doubly degenerate and each pair corresponding to one optical and one acoustic branch.

For the acoustic modes only, the $\gamma_{\mathbf{k}s}$ do not approach the same limits as **k** approaches zero from different directions; this causes no difficulty since at $\mathbf{k}=0$ the acoustic mode $\gamma_s$ are not physically significant. For each lattice, the curves of $\gamma_{\mathbf{k}s}$ for all the central potentials studied are qualitatively similar in shape.

## Low- and High-Temperature Quantities

The low-temperature quantities at $\sigma=0$ are listed in Table I. For a given central potential, it is seen that fcc and hcp quantities differ only on the order of 2%. The small values of $\bar{\theta}_{H0}/\kappa$ and $\gamma_{H0}$ for the bcc models reflect the small values of the velocities $c_s$ for one branch for **k** near the [011] direction. With the aid of (3.23), it is seen from Table I that the relative contribution of $V^2(d^2\bar{E}_H/dV^2)$ to the compressibility at $T=0$ and $\sigma=0$ is $\lesssim 15\kappa$ for all the models studied. This would represent a small contribution for most elements, since $\kappa\approx 10^{-3}$.

The high-temperature quantities at $\sigma=0$ are listed in Table II. For each central potential studied, the various Brillouin zone sums are nearly the same for fcc and hcp; consequently, it is not necessary

TABLE I. Thermodynamic quantities in the limit of low temperature, evaluated at $\sigma=0$. The error in $\kappa^{-1}V^2(d^2\bar{E}_H/dV^2)$ is no more than 1%; the error in other quantities is no more than 2 in the last place given.

| Model | $\bar{\theta}_{H0}/\kappa$ | $\gamma_{H0}$ | $V^2(d^2\bar{U}/dV^2)$ | $\kappa^{-1}V^2(d^2\bar{E}_H/dV^2)$ |
|---|---|---|---|---|
| fcc LJ(12,10) | 13.03 | 3.470 | 13.33 | 167 |
| fcc LJ(12,8) | 11.58 | 3.151 | 10.67 | 133 |
| fcc LJ(12,6) | 9.936 | 2.841 | 8.000 | 101 |
| fcc LJ(12,4) | 8.009 | 2.544 | 5.333 | 73.1 |
| fcc LJ(10,8) | 10.50 | 2.825 | 8.889 | 102 |
| fcc LJ(10,6) | 8.990 | 2.514 | 6.667 | 75.4 |
| fcc LJ(8,6) | 7.942 | 2.190 | 5.333 | 54.6 |
| fcc LJ(6,4) | 5.385 | 1.566 | 2.667 | 24.5 |
| hcp LJ(12,10) | 13.19 | 3.477 | hcp same as fcc within the stated accuracy. | |
| hcp LJ(12,8) | 11.73 | 3.154 | | |
| hcp LJ(12,6) | 10.09 | 2.836 | | |
| hcp LJ(12,4) | 8.152 | 2.529 | | |
| hcp LJ(10,8) | 10.65 | 2.824 | | |
| hcp LJ(10,6) | 9.145 | 2.506 | | |
| hcp LJ(8,6) | 8.099 | 2.177 | | |
| hcp LJ(6,4) | 5.527 | 1.535 | | |
| bcc LJ 6,4) | 2.907 | 2.004 | 2.667 | 23.3 |
| bcc R(1) | 2.014 | 0.4042 | 0.4532 | 1.58 |
| bcc R(2) | 3.406 | 0.8389 | 1.471 | 5.59 |
| bcc R(3) | 4.233 | 1.717 | 3.191 | 14.8 |

TABLE II. Quantities which determine the thermodynamic behavior at high temperature, evaluated at $\sigma=0$. The maximum errors are 1 in the last place given for $\bar{\theta}_{H\infty}/\kappa$, $d\ln\theta_{H\infty}/d\ln V$, $\gamma_{H\infty}$, and $\bar{\beta}_1$; 2% for $d\ln\gamma_{H\infty}/d\ln V$; 25% for $\bar{\beta}_2$, $\bar{\beta}_3$, and $\bar{\beta}_4$; and 10% for $\bar{\beta}_5$. Within these errors, the values for hcp are the same as for fcc, except for $\bar{\beta}_5$. The quantities needed to calculate $\bar{\beta}_5$ for fcc and hcp have been given previously.[2]

| Model | $\bar{\theta}_{H\infty}/\kappa$ | $\dfrac{d\ln\theta_{H\infty}}{d\ln V}$ | $\gamma_{H\infty}$ | $\dfrac{d\ln\gamma_{H\infty}}{d\ln V}$ | $\bar{\beta}_1$ | $\bar{\beta}_2$ | $\bar{\beta}_3$ | $\bar{\beta}_4$ | $\bar{\beta}_5$ |
|---|---|---|---|---|---|---|---|---|---|
| fcc LJ(12,10) | 11.73 | 3.765 | 3.690 | 1.30 | 0.8302 | 3.4 | −0.25 | 13 | 1.1 |
| fcc LJ(12,8) | 10.59 | 3.401 | 3.335 | 1.04 | 0.9380 | 3.3 | −0.04 | 13 | 1.1 |
| fcc LJ(12,6) | 9.313 | 3.014 | 2.964 | 0.709 | 1.111 | 3.3 | 0.32 | 12 | 1.1 |
| fcc LJ(12,4) | 7.841 | 2.581 | 2.559 | 0.283 | 1.439 | 3.3 | 1.0 | 11 | 1.2 |
| fcc LJ(10,8) | 9.746 | 3.050 | 2.989 | 0.903 | 1.009 | 3.0 | 0.10 | 11 | 0.95 |
| fcc LJ(10,6) | 8.603 | 2.665 | 2.619 | 0.627 | 1.179 | 2.9 | 0.44 | 9.6 | 0.91 |
| fcc LJ(8,6) | 7.837 | 2.308 | 2.269 | 0.510 | 1.276 | 2.5 | 0.62 | 7.3 | 0.70 |
| fcc LJ(6,4) | 6.019 | 1.543 | 1.531 | 0.139 | 1.722 | 1.3 | 1.5 | 2.3 | 0.15 |
| bcc LJ(6,4) | 5.890 | 1.541 | 1.544 | 0.155 | 1.737 | 0.74 | 1.5 | 1.3 | |
| bcc R(1) | 3.595 | 0.4117 | 0.3608 | 0.312 | 2.388 | | 1.6 | | |
| bcc R(2) | 4.940 | 0.8229 | 0.7841 | 0.522 | 1.599 | | 0.76 | | |
| bcc R(3) | 6.287 | 1.365 | 1.357 | 0.800 | 1.276 | | 0.26 | | |

to give the hcp values in Table II. The difference between $\gamma_{H\infty}$ and $-(d\ln\theta_{H\infty}/d\ln V)$ is generally small; the fact that these quantities are not equal has been pointed out by Barron.[13]

Certain of the present results may be compared with previous work. Barron[13] has calculated $\gamma_{H0}$ and $\gamma_{H\infty}$ for the fcc lattice for LJ(12,6), LJ(10,4), and LJ(8,6) potentials at $\sigma=0$. His values for $\gamma_{H0}$ agree with the present results within 1.5%; his $\gamma_{H\infty}$ are the same as the present values rounded to three significant figures. Barron and Klein[14] have calculated some quantities similar to $\bar{\theta}_{H\infty}/\kappa$ and $(d\ln\theta_{H\infty}/d\ln V)$ for the fcc LJ(12,6) model. Their calculations for $(r_0/r_1)^3=1.00$ (see their Table I) correspond to a $\sigma$-value, in the present notation, of 0.0296. The present results agree with those of Barron and Klein at this value of $\sigma$. Blackman[15] has found values of about 4.66 for $\gamma_{H0}$ and 4.89 for $\gamma_{H\infty}$ for a two-dimensional hexagonal lattice with LJ(12,6) potential; these values are much larger than the present results for hcp with the same potential.

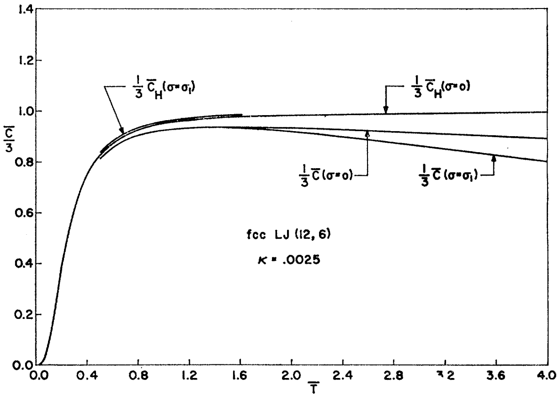

FIG. 7. Reduced specific heat at constant volume as a function of reduced temperature for fcc LJ(12,6) with $\kappa=0.0025$. $\bar{C}_H$ is the harmonic contribution and $\bar{C}$ is harmonic plus anharmonic contributions; $\sigma=0$ represents fixed volume and $\sigma=\sigma_1$ represents zero pressure.

## General Temperature Dependence

Figures 7–9 are representative graphs showing the temperature dependence of thermodynamic functions at constant volume ($\sigma=0$) and at constant pressure ($P=0$), with the explicit anharmonic contribution shown in each case. Certain approximations were made in obtaining these results. The explicit anharmonic corrections to $C$ and $\beta$ were not included at low temperatures; such corrections are too small to be represented on the graphs shown. At $\sigma=0$ the explicit anharmonic corrections were calculated by means of the high-temperature forms for $\bar{T}\geq 0.5$. In calculating the thermodynamic functions at zero pressure, the first step was to minimize the free energy with respect to $\sigma$ at each chosen temperature. The resulting $\sigma$, which corresponds to

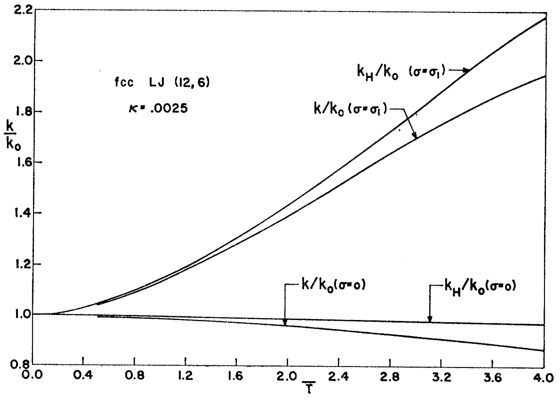

FIG. 8. Isothermal compressibility $k$, divided by $k_0=k(\bar{T}=0, \sigma=0)$, as a function of reduced temperature for fcc LJ(12,6) with $\kappa=0.0025$. $k_H$ is the harmonic contribution and $k$ is harmonic plus anharmonic contributions.

---

[13] T. H. K. Barron, Phil. Mag. 46, 720 (1955).

[14] T. H. K. Barron and M. L. Klein, Proc. Phys. Soc. (London) 82, 161 (1963).

[15] M. Blackman, Proc. Phys. Soc. (London) 74, 17 (1959).

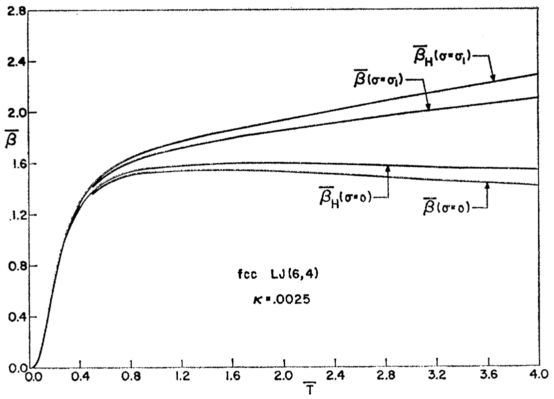

FIG. 9. Reduced thermal-expansion coefficient as a function of reduced temperature for fcc LJ(6,4) with $\kappa=0.0025$. $\bar{\beta}_H$ is the quasiharmonic contribution and $\bar{\beta}$ includes explicit anharmonic contributions; $\sigma=0$ represents fixed volume and $\sigma=\sigma_1$ represents zero pressure.

zero pressure, is denoted by $\sigma_1$. For $0\leq\bar{T}\leq 4$, the major contribution to the free energy is $F_H-NJE_H$; therefore this function was minimized to determine $\sigma_1$. The effect of including $NJE_H$ is to increase $\sigma_1$ by approximately $\kappa$, and the increase is nearly constant in temperature. The effect of including $F_A$ is to decrease $\sigma_1$, the decrease being negligible at $\bar{T}=0$ and of the order of $\kappa$ at $\bar{T}=4$. These minor corrections to $\sigma_1$ were neglected, since they lead to only minor changes in the graphs of the thermodynamic functions. An example of the temperature dependence of $\sigma_1$ is shown in Fig. 10. Finally the explicit anharmonic corrections to $C$ were calculated as functions of $(\sigma_1,\bar{T})$, while for $k$ and $\beta$ the explicit anharmonic corrections were taken to be the same at $\sigma=\sigma_1$ as at $\sigma=0$. The explicit anharmonic contributions were not calculated for the bcc models.

Certain general results of these model calculations may be summarized as follows. For each central potential studied, the set of curves for $\sigma_1$, $C$, $\beta$, and $k$ are very nearly the same for fcc and hcp. Also, at a given $\bar{T}$, $\sigma_1$ varies little with the lattice type or the potential considered, but is approximately proportional to $\kappa$. This behavior results in part from the fact that the ratio of the vibrational part of $F_H$ to the static part is proportional to $\kappa$ at any $\bar{T}$, just as at $\bar{T}=0$.[4] As is well known, the anharmonic specific heat is proportional to $T$ at high temperatures; more particularly, for the present models it is proportional to $\kappa\bar{T}$. Although the anharmonic specific heat is negative for fcc and hcp for the central potentials studied here, it may be expected to be of either sign for real materials. The difference between $C_H(\sigma=0)$ and $C_H(\sigma=\sigma_1)$ is quite small, and vanishes for $\bar{T}=0$ and $\bar{T}=\infty$; this behavior is to be expected. When anharmonicity is included, however, the difference between $C(\sigma=0)$ and $C(\sigma=\sigma_1)$ becomes observable on the graphs for $\bar{T}\approx 1$ and increases as $\bar{T}$ increases. The compressibility shows little temperature dependence at $\sigma=0$, and in particular the explicit anharmonic contribution is quite small. On the other hand, at $\sigma=\sigma_1$, the compressibility increases considerably with increasing $\bar{T}$, the explicit anharmonic contribution being still small. The behavior of the thermal-expansion coefficient is similar. $\beta_H$ for $\sigma=0$ shows little temperature dependence for $\bar{T}>1$, while for $\sigma=\sigma_1$, $\beta_H$ continues to increase considerably as $\bar{T}$ increases above 1; the explicit anharmonic contribution is small in each case.

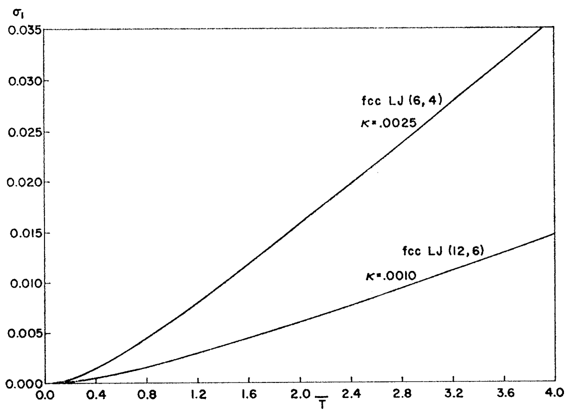

FIG. 10. Graphs of $\sigma_1$ as functions of reduced temperature for fcc LJ(6,4) with $\kappa=0.0025$ and for fcc LJ(12,6) with $\kappa=0.0010$.

### Effective Debye Temperatures

The effective Debye temperatures were computed from the specific heat values for all the models.[16] These results are illustrated by the curves of $\theta/\theta_{H0}$, Figs. 11 and 12. A wide variation of behavior was found for the different models. The large values of $\theta_H/\theta_{H0}$ for bcc at high $\bar{T}$ are due to the low values of $\theta_{H0}$, which are in turn due to the small values of some of the velocities $c_s$. In general, but not always, the longer range central potentials give rise to more complicated behavior at

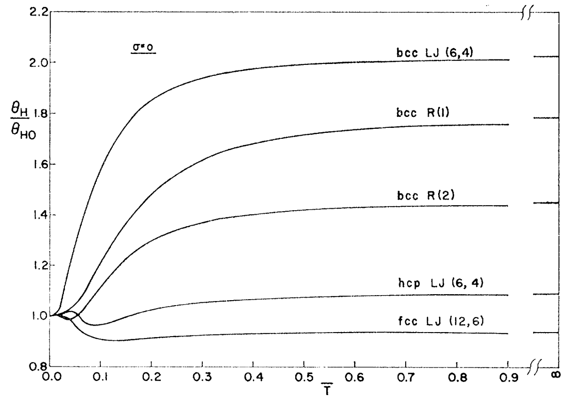

FIG. 11. Effective Debye temperatures for the harmonic specific heat at $\sigma=0$, plotted as $\theta_H/\theta_{H0}$, as functions of reduced temperature.

---

[16] Tables of the Debye function were kindly provided by Professor John R. Neighbours, U. S. Naval Postgraduate School, Monterey, California.

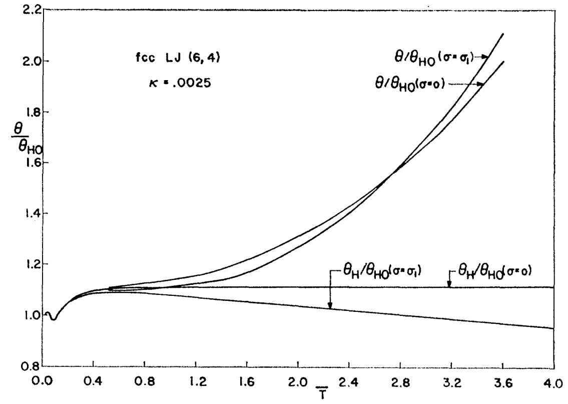

FIG. 12. Effective Debye temperature, plotted as $\theta/\theta_{H0}$, as a function of reduced temperature for fcc LJ(6,4) with $\kappa=0.0025$. $\theta_H$ is the Debye temperature for the harmonic specific heat and $\theta$ is the Debye temperature for the harmonic plus anharmonic specific heat.

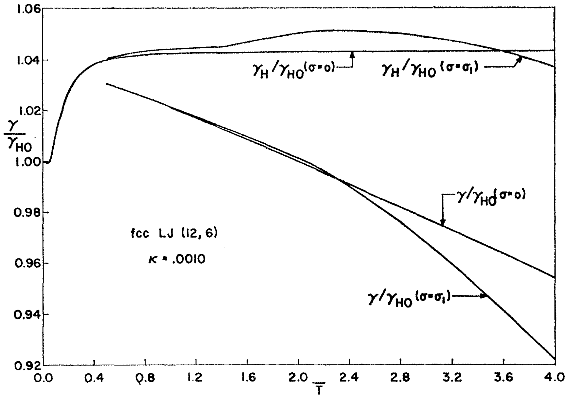

FIG. 14. Macroscopic Grüneisen parameter, plotted as $\gamma/\gamma_{H0}$, as a function of reduced temperature for fcc LJ(12,6) with $\kappa=0.0010$. $\gamma_H$ is the quasiharmonic Grüneisen parameter and $\gamma$ includes explicit anharmonic effects; $\sigma=0$ represents fixed volume and $\sigma=\sigma_1$ represents zero pressure.

low $\bar{T}$. The detailed behavior for $\bar{T}\lesssim 0.05$ was not determined in the present work; it may be more complicated than the graphs indicate. Horton and Leech[17] have recently calculated $\theta_H/\theta_{H0}$ for fcc for some Lennard-Jones potentials; the fcc LJ(12,6) curve of Fig. 11 is similar in shape to the curves which these authors have presented.

The negative anharmonic specific heat gives rise to a large increase in $\theta/\theta_{H0}$ with increasing $\bar{T}$, as shown in Fig. 12; for a positive anharmonic specific heat, $\theta/\theta_{H0}$ would decrease with increasing $\bar{T}$.

### Macroscopic Gruneisen Parameter

Some curves of $\gamma_H/\gamma_{H0}$ are shown in Fig. 13. The behavior is complicated, with large variations among the models. Barron[13] has pointed out that, for fixed volume, any variation in $\gamma_H$ should occur at temperatures of the order of $0.2\theta_{H0}$.

The explicit anharmonic corrections to $\gamma_T$ have been calculated for the fcc and hcp models at $\sigma=0$ and at $\sigma=\sigma_1$. For these models it was found that $\gamma_T$ always decreases from the value $\gamma_{H\infty}$ with increasing temperature, as shown in Fig. 14 for a particular model. This effect is complicated, even at $\sigma=0$. According to (2.24), the temperature variation of $\gamma_T$ is determined by the signs and relative magnitudes of $\beta_2$ and $\beta_5$. From Table II it is seen that $\beta_2$, $\beta_5$ are both positive and $\beta_2>\beta_5$; this leads to a decrease in $\gamma_T$ at $\sigma=0$. There is a larger relative decrease in $\gamma_T$ with increasing $\bar{T}$ at $\sigma=\sigma_1$. For real materials, however, $\gamma_T$ might be expected to increase or decrease with increasing temperature.

In Table II the volume derivative of $\gamma_{H\infty}$ is listed, as evaluated at $\sigma=0$; this derivative is positive in all cases. A characteristic of all the present models is that, as $\sigma$ increases, $\gamma_{H\infty}$ passes through a maximum at a small value of $\sigma$ and then decreases; this is illustrated in Fig. 15. Note that the curve of $\gamma_H/\gamma_{H0}$ at $\sigma=\sigma_1$, shown in Fig. 14, simply reflects the variation of $\gamma_{H\infty}$ with $\sigma$.

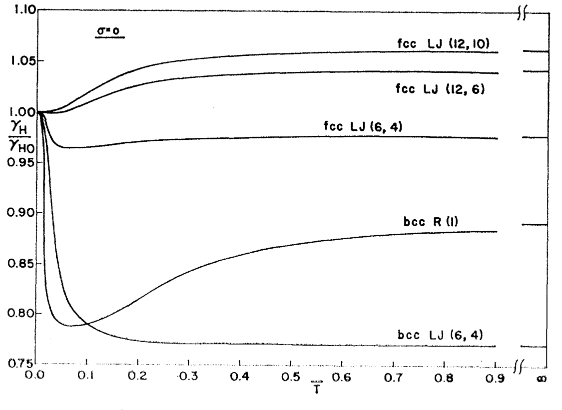

FIG. 13. Quasiharmonic Grüneisen parameters at $\sigma=0$, plotted as $\gamma_H/\gamma_{H0}$, as functions of reduced temperature.

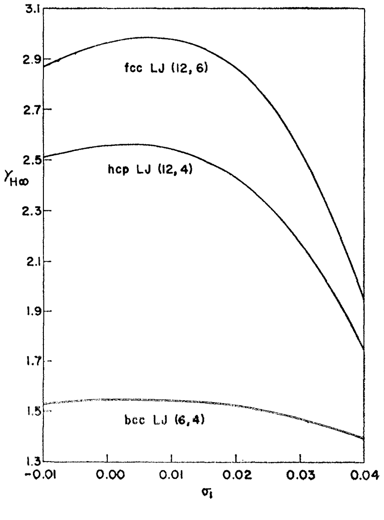

FIG. 15. High-temperature limit [illegible] of the quasiharmonic Gruneisen parameter as a function of $\sigma_1$ for some models.

---

[17] G. K. Horton and J. W. Leech, Proc. Phys. Soc. (London) 82, 816 (1963).

In consideration of Fig. 15, it is expected that for real materials the volume derivative of $\gamma_{H\infty}$ may be of either sign.

## V. APPROXIMATIONS

### Approximations to Accurate Expressions

It is of value to develop approximations which will allow the thermodynamic functions to be estimated with a small amount of labor. Approximations for some of the low- and high-temperature quantities are developed and tested in this section.

Consider an arbitrary initial configuration of the lattice, denoted by a tilde, with equilibrium positions $\tilde{\mathbf{r}}_{nj}$. A uniform volume change is represented by moving the ions to new positions $\mathbf{r}_{nj}$, where

$$\mathbf{r}_{nj}=(1+\xi)\tilde{\mathbf{r}}_{nj}, \quad \xi \text{ is small}. \tag{5.1}$$

The potential energy coefficients can be expressed as Maclaurin series in $\xi$[18]:

$$A_{n\rho,n'\rho'}=\tilde{A}_{n\rho,n'\rho'} +\xi \textstyle\sum_{n'',\rho''} \tilde{B}_{n\rho,n'\rho',n''\rho''}\tilde{r}_{n''\rho''}+\cdots, \tag{5.2}$$

with similar expansions for $B$ and $C$ coefficients. These expansions may then be used to obtain the volume derivatives of the potential energy coefficients, evaluated in the initial configuration.

If (1.5) is differentiated with respect to volume, and the resulting expression for $(d\omega_{\mathbf{k}s}/dV)$ is substituted into (2.25), the following equation is obtained for $\gamma_{H\infty}$.

$$\gamma_{H\infty}=-(6NJ)^{-1}\textstyle\sum_{\mathbf{k}}\sum_{\rho\rho'}(\mathbf{a}_{\mathbf{k}}^{-1})_{\rho'\rho} \times[V(d\mathbf{a}_{\mathbf{k}}/dV)_{\rho\rho'}], \tag{5.3}$$

where use has been made of the eigenvector expansion for the inverse dynamical matrix[2]:

$$\textstyle\sum_s v_{-\mathbf{k},\rho s}v_{\mathbf{k},\rho' s}(\omega_{\mathbf{k}s})^{-2}=M_c(\mathbf{a}_{\mathbf{k}}^{-1})_{\rho'\rho}. \tag{5.4}$$

Now a reasonably accurate approximation to the anharmonic free energy at high temperature has previously been obtained by replacing the inverse dynamical matrix by a diagonal matrix, according to[2]

$$a_{\mathbf{k},\rho\rho'}\approx\Omega\delta_{\rho\rho'}, \quad (\mathbf{a}_{\mathbf{k}}^{-1})_{\rho\rho'}\approx\Omega^{-1}\delta_{\rho\rho'}; \tag{5.5}$$

$$\Omega=(3NJ)^{-1}\textstyle\sum_{\mathbf{k}}\sum_{\rho} a_{\mathbf{k},\rho\rho}. \tag{5.6}$$

If (5.5) is used to replace $(\mathbf{a}_{\mathbf{k}}^{-1})_{\rho\rho'}$ in (5.3), and $V(d\mathbf{a}_{\mathbf{k}}/dV)_{\rho\rho'}$ is found with the aid of (5.2), remembering that $\mathbf{k}\cdot\mathbf{r}_{nj}$ is invariant under a uniform volume change, the approximation for $\gamma_{H\infty}$ becomes

$$\gamma_{H\infty}{}^{\dagger}=-(18J\Omega)^{-1}\textstyle\sum_{n,\rho\rho'} B_{0\rho,0\rho,n\rho'}r_{n\rho'}. \tag{5.7}$$

Throughout this section a dagger denotes an approximation. Since (5.7) has been obtained for an arbitrary initial configuration, the expression may be differentiated with respect to volume to give the result

$$(d\ln\gamma_{H\infty}{}^{\dagger}/d\ln V)=(2\gamma_{H\infty}{}^{\dagger}+\tfrac{1}{3})-(54J\Omega\gamma_{H\infty}{}^{\dagger})^{-1} \times\textstyle\sum_{nn',\rho\rho'\rho''} C_{0\rho,0\rho,n\rho',n'\rho''}r_{n\rho'}r_{n'\rho''}. \tag{5.8}$$

Approximate expressions for the anharmonic contributions to the free energy at high temperatures are given, in terms of $B$ and $C$ coefficients, by Eqs. (4.3) and (4.4) of Ref. 2.

When all masses are the same, $\Omega$ of (5.6) is the same as $\Omega_2$ of (3.18). The above method of approximating $\gamma_{H\infty}$ then leads to the result

$$\gamma_{H\infty}{}^{\dagger}=-(d\ln\theta_{H\infty}/d\ln V), \quad \text{when all } M_j=M. \tag{5.9}$$

The general treatment of the low-temperature limiting quantities is extremely complicated except for the case of primitive lattices. For a primitive lattice the values of $\gamma_s$, defined by (2.9), may be expected to show little variation from the mean; therefore, (2.8) is approximated here for primitive lattices by replacing each $\gamma_s$ by the average, denoted by $\Gamma$.

$$\Gamma=(12\pi)^{-1}\textstyle\sum_s \displaystyle\int d\Omega\,\gamma_s(\theta,\phi). \tag{5.10}$$

Furthermore, $\Gamma$ is approximated by a procedure analogous to the derivation of (5.7) above; the results are

$$\Gamma^{\dagger}=-\tfrac{1}{3}+(108\Lambda)^{-1}\textstyle\sum_{nn',ii'}B_{0i,ni,n'i'}\mathbf{r}_n{}^2r_{n'i'}, \tag{5.11}$$

$$\begin{aligned}\Lambda&=(12\pi)^{-1}\textstyle\sum_i \displaystyle\int d\Omega\,[\lambda(\theta,\phi)]_{ii},\\ &=-(1/18)\textstyle\sum_{n,i} A_{0i,ni}\mathbf{r}_n{}^2.\end{aligned} \tag{5.12}$$

Here $\Lambda$ is the average of the diagonal elements of the long-wavelength matrix $\lambda(\theta,\phi)$. The approximation for $\gamma_{H0}$ then becomes

$$\gamma_{H0}{}^{\dagger}=\tfrac{1}{3}+\Gamma^{\dagger}. \tag{5.13}$$

Approximate expressions for the anharmonic free energy at low temperatures for primitive lattices are given, in terms of $B$ and $C$ coefficients, by Eqs. (3.15) and (3.16) of Ref. 3.

For lattices with one or two ions per unit cell with all masses the same and with two-body central potentials, the approximations are simplified. The usual notation is used[2–4]: $\phi'_{0\nu}$ is the derivative of the central potential, with respect to $r^2$, evaluated at $r^2=r_\nu{}^2$; $\phi''_{0\nu}$ is the second derivative, and so forth. Some exact expressions, valid for any $\sigma$, are as follows:

$$dU/d\sigma=NJ\textstyle\sum_\nu r_\nu{}^2\phi'_{0\nu}, \tag{5.14}$$

$$d^2U/d\sigma^2=NJ\textstyle\sum_\nu [r_\nu{}^2\phi'_{0\nu}+2r_\nu{}^4\phi''_{0\nu}], \tag{5.15}$$

$$d^3U/d\sigma^3=NJ\textstyle\sum_\nu [6r_\nu{}^4\phi''_{0\nu}+4r_\nu{}^6\phi'''_{0\nu}], \tag{5.16}$$

$$\Omega=\Omega_2=\textstyle\sum_\nu [2\phi'_{0\nu}+(4/3)r_\nu{}^2\phi''_{0\nu}], \tag{5.17}$$

$$\Lambda=(1/9)\textstyle\sum_n [3r_n{}^2\phi'_{0n}+2r_n{}^4\phi''_{0n}], \tag{5.18}$$

---

[18] See, for example, R. E. Peierls, *Quantum Theory of Solids* (Clarendon Press, Oxford, England, 1955).

where $\Lambda$ is for primitive lattices only. The approximations are summarized below.

$$\gamma_{H\infty}{}^{\dagger}=-(2/9\Omega)\sum_{\nu}[5r_{\nu}{}^{2}\phi''{}_{0\nu}+2r_{\nu}{}^{4}\phi'''{}_{0\nu}], \quad (5.19)$$

$$d\ln\gamma_{H\infty}{}^{\dagger}/d\ln V)=(2\gamma_{H\infty}{}^{\dagger}+\tfrac{1}{3})-(2/27\Omega\gamma_{H\infty}{}^{\dagger}) \times\sum_{\nu}[5r_{\nu}{}^{2}\phi''{}_{0\nu}+16r_{\nu}{}^{4}\phi'''{}_{0\nu}+4r_{\nu}{}^{6}\phi^{\mathrm{iv}}{}_{0\nu}], \quad (5.20)$$

$$\gamma_{H0}{}^{\dagger}=-(1/27\Lambda)\sum_{n}[5r_{n}{}^{4}\phi''{}_{0n}+2r_{n}{}^{6}\phi'''{}_{0n}], \quad (5.21)$$

$$G_3{}^{\dagger}=-(4NJK^2/\Omega^3)\sum_{\nu}[15r_{\nu}{}^{2}(\phi''{}_{0\nu})^2 +12r_{\nu}{}^{4}\phi''{}_{0\nu}\phi'''{}_{0\nu}+4r_{\nu}{}^{6}(\phi'''{}_{0\nu})^2], \quad (5.22)$$

$$G_4{}^{\dagger}=(NJK^2/\Omega^2)\sum_{\nu}[15\phi''{}_{0\nu} +20r_{\nu}{}^{2}\phi'''{}_{0\nu}+4r_{\nu}{}^{4}\phi^{\mathrm{iv}}{}_{0\nu}], \quad (5.23)$$

where

$$G^{\dagger}=G_3{}^{\dagger}+G_4{}^{\dagger}. \quad (5.24)$$

In extending the original approximations for $G_3$ and $G_4$ to all neighbors and all lattices with one or two ions per unit cell, the small contribution from the $(B_{0i,0i',0i''})^2$ terms, Eq. (4.5) of Ref. 2, has been dropped.

As mentioned in Sec. III above, the expressions (5.22) and (5.23) were used to calculate (approximately) the volume derivatives of $G$. The results are given in Table III for fcc; the values for hcp are identical to the number of figures given. The various derivatives of $G_3{}^{\dagger}$ and $G_4{}^{\dagger}$ are not listed in Table III. For each potential, it was found that $(V/G_3{}^{\dagger})(dG_3{}^{\dagger}/dV)\approx(V/G_4{}^{\dagger})(dG_4{}^{\dagger}/dV)$, and similarly for second derivatives. As a result, the derivatives of $G^{\dagger}$ listed in Table III are believed to represent derivatives of $G$ as accurately as $G^{\dagger}$ represents $G$.[2]

The expressions (5.14)–(5.23) are easily transformed to simple forms involving the lattice sums which are tabulated in an Appendix of Ref. 4. With the aid of these sums the approximations were evaluated at $\sigma=0$ for the models. Note that $(dU/d\sigma)=0$ at $\sigma=0$. The results of comparing the approximations with the accurate values are given in Table IV in the form of the errors $\delta Q$, where for any quantity $Q$ whose approximation is $Q^{\dagger}$,

$$\delta Q=(Q-Q^{\dagger})/Q. \quad (5.25)$$

The hcp results are not listed since for high-temperature quantities the approximations and errors are essentially the same as for fcc, while the low-temperature approximations have not been treated for hcp. The approximations are in general quite satisfactory, except for the case of bcc R(1), where the error in each quantity is much larger than for any other model. The unusual properties of this model are evident throughout the present work, and appear to be due to the fact that this potential varies much less with distance out to the third neighbors than do the other potentials for the bcc and other lattices.

The further approximation of taking only the nearest-neighbor contributions to the sums in (5.14)–(5.23) has also been investigated. This procedure nearly always increases the error of the approximation, and by a large amount in all cases but the very short-range potentials.

TABLE III. Volume derivatives of the approximate coefficient of the anharmonic free energy at high temperature, evaluated at $\sigma=0$. For each potential, the values for hcp are the same as for fcc.

| Model | $(V/G^{\dagger})(dG^{\dagger}/dV)$ | $(V^2/G^{\dagger})(d^2G^{\dagger}/dV^2)$ |
|---|---|---|
| fcc LJ(12,10) | 8.52 | 80.1 |
| fcc LJ(12,8) | 7.50 | 60.8 |
| fcc LJ(12,6) | 6.33 | 41.3 |
| fcc LJ(12,4) | 4.88 | 21.7 |
| fcc LJ(10,8) | 6.55 | 47.5 |
| fcc LJ(10,6) | 5.58 | 31.4 |
| fcc LJ(8,6) | 4.77 | 22.2 |
| fcc LJ(6,4) | 2.75 | 5.61 |

TABLE IV. Errors in the approximations (5.19)–(5.21), evaluated at $\sigma=0$. The errors are expressed according to the definition (5.25).

| Model | $\delta\gamma_{H\infty}$ | $\delta(d\ln\gamma_{H\infty}/d\ln V)$ | $\delta\gamma_{H0}$ |
|---|---|---|---|
| fcc LJ(12,10) | −0.020 | −0.035 | −0.105 |
| fcc LJ(12,8) | −0.020 | −0.044 | −0.111 |
| fcc LJ(12,6) | −0.017 | −0.071 | −0.115 |
| fcc LJ(12,4) | −0.009 | −0.071 | −0.114 |
| fcc LJ(10,8) | −0.020 | −0.054 | −0.121 |
| fcc LJ(10,6) | −0.018 | −0.059 | −0.127 |
| fcc LJ(8,6) | −0.017 | −0.061 | −0.141 |
| fcc LJ(6,4) | −0.008 | −0.065 | −0.171 |
| bcc LJ(6,4) | 0.002 | 0.058 | 0.085 |
| bcc R(1) | −0.141 | 0.138 | −0.555 |
| bcc R(2) | −0.050 | 0.080 | −0.177 |
| bcc R(3) | −0.006 | 0.088 | 0.131 |

## Relations Between Anharmonic Properties

With the aid of (5.14)–(5.23) it is possible to find simple approximate relations between different anharmonic properties. This has been carried out with the consistent use of further approximations of the type

$$\epsilon^2\sum_{\nu}r_{\nu}{}^{2}\phi''{}_{0\nu}\approx\sum_{\nu}r_{\nu}{}^{4}\phi''{}_{0\nu}. \quad (5.26)$$

Note that this relation is correct for the nearest-neighbor contributions. The only difficulty arises for the quantity $G_3{}^{\dagger}$; the expression (5.22) is handled by rewriting the last term according

$$\sum_{\nu}r_{\nu}{}^{6}(\phi'''{}_{0\nu})^2\approx z^{-1}[\sum_{\nu}r_{\nu}{}^{3}\phi'''{}_{0\nu}]^2, \quad (5.27)$$

where $z$ is the number of nearest neighbors. This approximation is correct for the nearest-neighbor contributions. The first two terms in (5.22), involving $(\phi''{}_{0\nu})^2$ and $\phi''{}_{0\nu}\phi'''{}_{0\nu}$, are small; these terms are neglected since this procedure, coupled with the use of (5.27), is found empirically to give a good approximation.

With the aid of (5.26), it is found for $\sigma=0$

$$\Omega\approx(6V_a/\epsilon_0{}^2k_0). \quad (5.28)$$

This is not a good approximation for the present models, the error varying from very small for the short-range potentials to ~30% for the long-range potentials. Nevertheless, the consistent use of (5.28) to eliminate $\Omega$ does not seriously affect the final approximations. The relations between anharmonic properties were trans-

TABLE V. Errors in the approximations (5.29)–(5.31), evaluated at $\sigma=0$. The errors are expressed according to the defintion (5.25) and discussion in the text.

| Model | $\delta(d\ln k_0/d\ln V)$ | $\delta\beta_{Ht}$ | $\delta(C_{AT}/NJK)$ |
|---|---|---|---|
| fcc LJ(12,10) | 0.006 | −0.061 | −0.190 |
| fcc LJ(12,8) | 0.014 | −0.058 | −0.191 |
| fcc LJ(12,6) | 0.027 | −0.045 | −0.194 |
| fcc LJ(12,4) | 0.051 | −0.012 | −0.190 |
| fcc LJ(10,8) | 0.023 | −0.058 | −0.188 |
| fcc LJ(10,6) | 0.038 | −0.045 | −0.185 |
| fcc LJ(8,6) | 0.052 | −0.042 | −0.201 |
| fcc LJ(6,4) | 0.100 | 0.002 | −0.617 |
| bcc LJ(6,4) | 0.096 | 0.229 | |

formed so as to contain easily measured quantities and applied at $\sigma=0$. After a lot of algebra, the results are

$$(d\ln k_0/d\ln V)\approx\tfrac{2}{3}(b+\tfrac{5}{2})\,, \tag{5.29}$$

$$\beta_{Ht}\approx(4\pi^4/5)(\beta_1/\theta_{H0}{}^3)T^3\,, \tag{5.30}$$

$$\begin{aligned}C_{AT}/NJK\approx\{&(3\beta_1/zb)(b+\tfrac{5}{2})^2\\&-2\beta_1[b-\tfrac{3}{4}(d\ln\beta_1/d\ln V)+\tfrac{1}{4}]\}T\,,\end{aligned} \tag{5.31}$$

where

$$b=(V_a\beta_1/Kk_0)\,. \tag{5.32}$$

In obtaining (5.30), a preliminary result was

$$\gamma_{H0}\approx\gamma_{H\infty}; \tag{5.33}$$

this has been derived for primitive lattices only and is a fair approximation for the present models.

The errors in (5.29)–(5.31) may be represented according to the definition (5.25), where the right-hand side is considered an approximation to the quantity on the left. These errors are listed in Table V for the present models at $\sigma=0$. In view of their simplicity, the approximations are considered satisfactory.

## VI. DISCUSSION

The present paper, as well as previous work,[2–4] reports the results of extensive numerical calculations of thermodynamic properties of crystals. These calculations are based on the lattice-dynamics free energy, for models with prescribed interactions among the ions. Direct summation over a portion of the Brillouin zone, with the use of weighting factors, is a much more practical method of carrying out such calculations than is the more customary method of calculating the frequency-distribution function, transforming Brillouin zone sums to frequency integrals, and then integrating over frequencies. In addition, the Hellmann-Feynman theorem provides a convenient method of obtaining the first derivatives of the eigenvalues with respect to configuration.

Since the accurate calculation of thermodynamic functions for a specified model is generally tedious, it is desirable to be able to estimate such quantities. The accurate calculations of the present and previous work may serve as references for checking such approximations as may be developed. In addition, the approximations which have been developed may serve to estimate anharmonic-thermodynamic functions for models in which the interactions among the ions are specified.

The thermodynamic properties of the central-potential models exhibit certain qualitative features which may be expected to describe many real materials. The harmonic contribution to the specific heat approaches a constant value at high temperatures for fixed volume ($\sigma=0$) or for zero pressure ($\sigma=\sigma_1$). On the other hand, the explicit anharmonic contribution at high temperature, which is proportional to $T$ at $\sigma=0$, is not negligible in general, and may have a strong volume dependence. At $\sigma=0$ the isothermal compressibility has only a small temperature dependence and the explicit anharmonic contribution is small, while at $\sigma=\sigma_1$ the compressibility increases considerably with increasing temperature, again with the anharmonic contribution being small. At $\sigma=0$ the quasiharmonic thermal-expansion coefficient has only a small temperature dependence at high temperatures, and the explicit anharmonic contribution is small. On the other hand, at $\sigma=\sigma_1$ the thermal-expansion coefficient increases considerably with increasing temperature at high temperature, while the explicit anharmonic contribution is again small. This temperature dependence of $k$ and $\beta$ at $\sigma=0$ and at $\sigma=\sigma_1$ reflects the large volume dependence, and small explicit temperature dependence, of these quantities. At $\sigma=0$ the quasiharmonic Gruneisen parameter approaches a constant value at high temperatures; the departure from this high temperature limit at $\sigma=\sigma_1$, and the explicit anharmonic corrections at $\sigma=0$ and $\sigma=\sigma_1$, are complicated and are not negligible in general.

The approximate relations between anharmonic properties, as given by (5.29)–(5.31), might be of value in estimating an anharmonic property of a material with the aid of other properties of the material. In view of the derivation of these relations, they may be expected to apply only to elements in the crystalline state, and then only qualitatively.

An extensive study of the available data for many materials is presently being carried out. This study includes the reduction of $C$, $\beta$, and $k$, as measured at zero pressure, to a fixed volume. Preliminary results indicate that the temperature dependence of these thermodynamic quantities, at fixed volume and at zero pressure, agrees qualitatively with behavior summarized above for the present calculations, at $\sigma=0$ and at $\sigma=\sigma_1$, respectively. In addition, the relations (5.29)–(5.31) appear to hold qualitatively for the elements.